eNeuro

Research Article: New Research | Disorders of the Nervous System

Distinct temporal structure of nicotinic ACh receptor activation determines responses of VTA neurons to endogenous ACh and nicotine

https://doi.org/10.1523/ENEURO.0418-19.2020

Cite as: eNeuro 2020; 10.1523/ENEURO.0418-19.2020

Received: 10 October 2019
Revised: 10 February 2020
Accepted: 18 April 2020

Distinct temporal structure of nicotinic ACh receptor activation determines responses of VTA neurons to endogenous ACh and nicotine

Abbreviated Title: **VTA responses to endogenous ACh and nicotine**

E. Morozova[1], P. Faure[2], B. Gutkin[3,4], C. Lapish[5,7], A. Kuznetsov[6,7].

[1] Volen Center for Complex systems, Brandeis University, Waltham 02453

[2] Neuroscience Paris Seine – Institut de Biologie Paris Seine (NPS – IBPS), Sorbonne Université, INSERM, CNRS, Paris, France 75013

[3] Group for Neural Theory, LNC2 INSERM U960, DEC, Ecole Normale Supérieure PLS* University, Paris, France 75005

[4] Center for Cognition and Decision Making, Institute for Cognitive Neuroscience, NRU Higher School of Economics, Moscow Russia 101000

[5] Department of Psychology, Indiana University-Purdue University at Indianapolis, 46204

[6] Department of Mathematical Sciences, Indiana University-Purdue University at Indianapolis 46204

[7] Indiana Alcohol Research Center, Indiana University School of Medicine, Indianapolis 46204

Corresponding author: Alexey Kuznetsov askuznet@iupui.edu

Author contributions: EM designed an coded the model and wrote the text. PF provided the experimental data, and edited the text, BG interpreted the results and edited the text, CL edited the text, AK lead the project, designed the model and wrote the text.

Number of pages: 40

Number of figures 7, tables 2

22 **Number of words: abstract 249, introduction 652, discussion 1486.**

23 **Conflict of interests: The authors declare no competing financial interests.**

24 **Acknowledgments:** The author acknowledge the following support: the French National Cancer
25 Institute Grant TABAC-16-022 (P.F.), the Agence Nationale de la Recherche (ANR) and the
26 LabEx Bio-Psy (P.F.)

27

Distinct temporal structure of nicotinic ACh receptor activation determines responses of VTA neurons to endogenous ACh and nicotine

Abbreviated Title: **VTA responses to endogenous ACh and nicotine**

Abstract

The addictive component of tobacco, nicotine, acts through nicotinic acetylcholine receptors (nAChRs). The β2 subunit-containing nAChRs (β2-nAChRs) play a crucial role in the rewarding properties of nicotine and are particularly densely expressed in the mesolimbic dopamine (DA) system. Specifically, nAChRs directly and indirectly affect DA neurons in the ventral tegmental area (VTA). Understanding of ACh and nicotinic regulation of DA neuron activity is incomplete. By computational modeling, we provide mechanisms for several apparently contradictory experimental results. First, systemic knock out of β2-containing nAChRs drastically reduces DA neurons bursting even though the major glutamatergic (Glu) afferents that have been shown to evoke this bursting stay intact. Second, the most intuitive way to rescue this bursting - by re-expressing the nAChRs on VTA DA neurons - fails. Third, nAChR re-expression on VTA GABA neurons rescues bursting in DA neurons and increases their firing rate under the influence of ACh input, whereas nicotinic application results in the opposite changes in firing. Our model shows that, first, without ACh receptors Glu excitation of VTA DA and GABA neurons remain balanced and cancel each other. Second, re-expression of ACh receptors on DA neurons provides an input that impedes membrane repolarization and is ineffective in restoring firing of DA neurons. Third, the distinct responses to ACh and nicotine are due to distinct temporal patterns of these inputs: pulsatile vs. continuous. Altogether this study highlights how β2-nAChRs influence co-activation of VTA DA and GABA neurons required for motivation and saliency signals carried by DA neuron activity.

Significance statement

Tobacco use remains the worldwide leading cause of preventable mortality. Nicotine, the addictive component of tobacco, exerts its effects through nicotinic acetylcholine receptors (nAChRs). The central dopamine (DA) system, and particularly DA release by neurons contained in ventral tegmental area (VTA) is shown to play a central role in developing addictions. Understanding of ACh and nicotinic regulation of DA neuron activity is incomplete, and here we resolve several apparently contradictory experimental results. In particular, we show that distinct responses to ACh and nicotine observed in certain experiments are due to distinct temporal patterns of these inputs: pulsatile vs. continuous. This distinction highlights how motivation and saliency signals carried by DA signaling are hijacked by nicotine and other addictive drugs.

Introduction

As more than five million smokers die every year from the consequences of tobacco use, it remains the worldwide leading cause of preventable mortality (CDCTobaccoFree, 2017). Underlying neurobiological mechanisms of tobacco dependence have been extensively explored (Taly et al., 2009; Changeux, 2010; Benowitz, 2010, 2009), but remain far from being understood at the neural circuit level. Nicotine, the addictive component of tobacco (Marti et al., 2011), acts through nicotinic acetylcholine receptors (nAChRs) (Role and Kandel, 2008). Among the different nAChRs, the β2-containing nAChRs (β2-nAChRs) play a crucial role in positive rewarding properties of nicotine (Picciotto et al., 1998; Durand-de Cuttoli et al., 2018) and is particularly densely expressed in the mesolimbic reward system (Klink et al., 2001).

The mesolimbic reward system and, specifically, reward-related dopamine (DA) release throughout the brain plays a major role in addictive and drug-seeking behaviors (Koob et al., 1998; Everitt and Robbins, 2005; Keiflin and Janak, 2015). DA-releasing neurons have two major modes of activity: nearly-tonic background firing and bursting. Background firing is responsible for the basal DA levels in the projection areas and is altered in psychiatric disorders from depression to schizophrenia (Grace, 1991; Nestler and Carlezon, 2006). Phasic DA changes, caused by DA neuron burst firing follow external stimuli and are suggested to serve as motivational, saliency and unexpected reward signals (Schultz, 2002; Redgrave and Gurney, 2006). Bursting mode of the DA neuron is associated with an increase in occurrence of the behavior that preceded the burst by the mechanism called reinforcement learning (Bayer and Glimcher, 2005; Keiflin and Janak, 2015). DA neurons are contained in the VTA together with γ-aminobutyric acid (GABA) neurons. Most drugs of abuse alter DA levels either directly though receptor binding (Lüscher and Ungless, 2006), or indirectly by acting on VTA GABA neurons

85 (Steffensen et al., 2011; Bocklisch et al., 2013). Nicotine influence is very complex to analyze
86 since it enhances DA release by acting on multiple targets on both VTA DA and GABA neurons
87 (Tolu et al., 2013; Faure et al., 2014). Mechanisms of nicotinic influence proposed in previous
88 studies (Mansvelder et al., 2002; Mao et al., 2011) could not explain why, for example, repeated
89 nicotine injections cause excitation of the GABA neurons and yet increase DA release.
90 Therefore, there is a gap in understanding the complex interaction of VTA DA and GABA
91 neurons, which we address through data-based computational modeling.

92 β2-nAChRs are expressed on both VTA DA and GABA neurons. Systemic deletion of the
93 receptors eliminates bursting mode of DA neurons (Mameli-Engvall et al., 2006) (Fig. 1A). Such
94 DA neuron bursting is in turn implicated in reinforcement (Bayer and Glimcher, 2005; Keiflin
95 and Janak, 2015). The role of β2-nAChRs on DA or GABA neurons in nicotine reinforcement
96 (i.e. an increase in nicotine consumption) was addressed in previous papers using re-expression
97 of the β2-nAChRs in specific cell populations of the VTA. It has been shown that a global re-
98 expression of the β2- nAChRs in all the VTA (Mameli-Engvall et al., 2006; Naudé et al., 2016)
99 augmented DA neuron firing rate and burstiness compared to β2 KO mice (Fig 1B – C purple vs.
100 red). Activation of β2-nAChRs by ACh specifically on the VTA GABA neurons results in
101 increased firing and, importantly, augmented burstiness of DA neurons (Fig. 1D, blue vs. red).
102 By contrast, activation of these receptors expressed only on DA neurons by ACh does not
103 produce this effect (Fig. 1D, green).

104 Adding to the complexity, exposing β2-nAChRs to nicotine produces different effects (data
105 summarized in Fig. 2): In the case of receptors re-expression on the GABA neurons, nicotine
106 increases GABA neuron firing rates and, consecutively, decreases the DA neuron firing rate and
107 bursting (Fig. 2 blue), in contrast to baseline conditions with endogenous ACh input. Nicotine

acting through nAChRs expressed only on DA neurons significantly increases DA neuron firing rate, but not bursting (Fig. 2 green, (Tolu et al., 2013)). Finally, if the receptors are expressed on all VTA neurons (Mameli-Engvall et al., 2006; Tolu et al., 2013; Naudé et al., 2016), nicotine robustly increased firing rate and bursting of DA neurons (Fig. 2 purple, (Naudé et al., 2016)). Attempts to explain this bidirectional modulation heuristically, for example by receptor desensitization, have not been successful. We turn to computational modelling to clarify this apparent conundrum. In this paper, we analyze the role of local interactions between DA and GABA neurons that mediate the influence of β2-nAChR on the key properties of the DA neuron activity.

By computational modeling, we (1) reconcile the increase of VTA DA cell activity under endogenous ACh with its nicotine-evoked suppression when β2-nAChRs are re-expressed only on the VTA GABA neurons; (2) show why receptor re-expressions restricted to the DA or GABA neurons do not restore nicotine impact on the DA firing to levels seen in wild type (WT) animals, while re-expression in all VTA neurons does.

Methods

VTA network:

The model network consists of a DA neuron innervated by a population of GABA neurons (Fig. 3A). The DA neuron received Glu excitatory input, and both DA and GABA neurons receive cholinergic input via nACh receptors. There are other inputs to this circuit, for example from the nucleus accumbens, but experiments show that re-expression only in the VTA (on all VTA cells) restores all the differences observed in β2-/- knockout (Naudé et al., 2016). Therefore, these afferents are unlikely to be responsible for the observed differences. Thus, other inputs are

omitted in the model. The biophysical models of the DA and GABA neurons are conductance-based one-compartmental models modified from (Morozova et al., 2016a) by adding nAChR currents:

$$c_m \frac{dv_{DA}}{dt} = I_{Ca} + I_{KCa} + I_K + I_{DR} + I_{Na} + I_{sNa} + I_{leak} + I_h + I_{NMDA} + I_{AMPA} + I_{GABA} + I_{AChDA}$$

$$c_m \frac{dv_{GABA}}{dt} = I_K + I_{Na} + I_{leak} + I_{AChGABA}$$

For complete description of the model, see Morozova et al. (2016). Briefly, The first eight currents in the DA neuron equation are intrinsic: calcium, calcum-dependent potassium (SK), subthreshold potassium, spike-producing potassium delayed rectifier and sodium, subthreshold sodium, leak and hyperpolarization-activated cationic current (H). The rest of the currents are synaptic: NMDA, AMPA, $GABA_A$ and nACh receptors. The GABA neuron includes only spike-producing sodium and potassium, and the leak intrinsic currents, and the nACh receptor curent. Gating variables for all currents are modeled in the standard form $\frac{dX}{dt} = \frac{X_{inf}(V)-X}{\tau_X}$, where X denotes a specific gating varible, $X_{inf}(V)$ is the function of its steady state activation, and τ_X is its time constant. The model has been calibrated using in vitro and in vivo data in the previous publications (see (Morozova et al., 2016a, 2016b)). We list the values for all parameters in extended data Table 1-1 and refer the reader to the above publications for detailed explanations.

Cholinergic currents:

We modeled only the nAChR currents on VTA neurons because other currents affected by cholinergic inputs are not changed in the KO conditions, and, thus, cannot cause the observed differences. The nAChR currents on DA and GABA neurons are given by the following expressions respectivelly: $I_{AChDA} = g_{AChDA}(E_{ACh} - v_{DA})$ and $I_{AChGABA} = g_{AChGABA}(E_{ACh} - v_{GABA})$.

Here, $E_{ACh} = 0$. The model of nAChR activation and desensitization was adapted from (Graupner et al., 2013). Note that the approach has been also validated and used to partially explain data in (Tolu et al., 2013). The model for the nAChR-mediated currents has four different states of the nAChR: deactivated/sensitized (also resting or responsive state), activated/sensitized, activated/desensitized and deactivated/desensitized state (Graupner et al., 2013). The mean total activation level of nAChRs is a product of the fraction of receptors in the activated state Ach_{act} and the fraction of reseptors in the sensitized state $(1 - ACh_{des})$, thus, conductance of the cholinergic current is given by $g_{Ach} = \bar{g}_{Ach} \cdot Ach_{act} \cdot (1 - Ach_{des})$. The time course of the activation and desensitization variables is given by $\frac{dACh_{act}}{dt} = \frac{ACh_{act\infty} - ACh_{act}}{\tau_{ACh_{act}}}$ and $\frac{dACh_{des}}{dt} = \frac{ACh_{des\infty} - ACh_{des}}{\tau_{ACh_{des}}}$ respectively. $\tau_{ACh_{act}} = 5ms$ is an activation time constant, $\tau_{ACh_{des}} = 500 + 6 \cdot 10^5 \cdot \frac{1}{1 + (\frac{inp_{Nic}}{K_\tau})^3} ms$ is a nicotine concentration-dependent desensitization time constant. Steady states $Ach_{act\infty}$ and $Ach_{des\infty}$ are given by Hills equations of the form $Ach_{act} = \frac{1}{(1 + (\frac{EC_{50}}{inp_{Ach} + w \cdot inp_{Nic}})^{1.05})}$ and $Ach_{des} = \frac{1}{(1 + (\frac{IC_{50}}{inp_{Nic}})^{0.5})}$. Here, EC_{50} and IC_{50} are the half-maximal concentrations of nAChR activation and desensitization respectively. w is the potency of nicotine to evoke a response. The parameters for the cholinergic currents were calibrated in previous publications (Graupner et al., 2013; Tolu et al., 2013). We refer the reader to these publications for detailed explanations and list the values in Extended data Table 1-1, except for the parameters recalibrated in this study listed in Tables 1 and 2.

Nicotine has relatively slow pharmacodynamics in the brain, hence the application of nicotine was modeled as slow increase in inp_{nic} causing slow activation of the nAChRs followed by yet slower desensitization. On the other hand, endogenous cholinergic input to the VTA was temporally structured as a spike train with a bimodal distribution to achieve bursty firing pattern. The majority of neurons in laterodorsal tegmental nucleus (LTDg) and pedunculopontine tegmental nucleus (PPTg) are generally slow, maintaining individual firing rates averages between 2 and 5 Hz (Sakai, 2012; Kayama et al., 1992). Putative cholinergic neurons transiently increase their firing rate reaching 10 Hz in response to sensory stimuli (Koyama et al., 1994). It has been shown that LTDg neurons are essential for DA neuron burst firing. However, microiontophoretically applied acetylcholine onto identified DA neurons, while inactivating the LDTg, failed to induce burst firing in DA neurons (Lodge and Grace, 2006). This likely suggests that temporal structure of cholinergic input onto VTA neurons is crucial for DA neuron burst firing. The number of these afferent neurons converging to each VTA neuron is not known. We assume this number to be in the range of 20-60 suggested for other subcortical afferents. Multiplying the number of afferent neurons by the rate, under the assumption that the projecting neurons are asynchronous, gives us the average ACh afferent input frequencies of 60-180 Hz. If ACh afferents are synchronized, these rates will be lower, whereas the amplitude of this input will be greater. Thus, we position the peaks of the frequency distributions for ACh input at 3.3 and 30 Hz (i.e. interspike intervals of 300 and 30 ms). The ACh input spiketrain was generated by drawing the interspike intervals from the two normal distributions with standard deviation 7Hz and their relative contributions of 0.7 and 0.3 for 30 and 3.3 Hz respectively (Fig. 3B).

Assuming that the intravenous nicotine concentration slowly builds up at the site of the receptor, it increases and then decays exponentially in the model with a rise time constant of 0.5 min and decay time constant of 3 min (Fig. 3C):

$$inp_{Nic} = Ainp_{Nic}(e^{-\frac{t}{\tau_{rise}}} - e^{-\frac{t}{\tau_{decay}}})$$

The amplitude of the nicotinic input $Ainp_{nic}$ is assumed to be lower by a factor of 10 than that of ACh (Table 1) because, by contrast to nicotine, ACh is released locally at the synapse. The concentrations match those projected from experiments (Garzón et al., 1999). The model is coded in MATLAB/c++, and the code is available on ModeDB database.

Table 1: Model parameters (see Extended data Table 1-1 for full list)

Parameter	Description	DA neuron	GABA neuron
$Ainp_{Ach}$	Amplitude of Ach input	5 uM	10 uM
$Ainp_{Nic}$	Amplitude of Nic input	0.5 uM	0.5 uM
w	Potency of Nic to evoke response	3	3
g_{GABA}	GABAR conductance	2.5 mS/cm^2	-
g_{NMDA}	NMDAR conductance	4 mS/cm^2	0 mS/cm^2
g_l	Leak conductance	0.03 mS/cm^2	0.05+0.05(rnd-0.5) mS/cm^2

Table 2: ACh receptor maximal conductance used to reproduce different KO-re-expression cases

Parameter	KO	Re-expression on DA	Re-expression on GABA	Re-expression on both, WT case

$\bar{g}_{AChDA}$	0	$5\ mS/cm^2$	0	$10\ mS/cm^2$
$\bar{g}_{AChGABA}$	0	0	$4\ mS/cm^2$	$1.5\ mS/cm^2$

DA neuron firing pattern quantification

According to the classical definition (Grace and Bunney, 1984), bursts were identified as discrete events consisting of a sequence of spikes with burst onset defined by two consecutive spikes within an interval less than 80 msec, and burst termination defined by an interspike interval greater than 160 msec. To quantify bursting we used the % of spikes within burst (%SWB), calculated as the number of spikes within bursts divided by the total number of spikes. In our simulations, the majority of bursts were composed of doublets; this is consistent with data (Grace and Bunney, 1984; Mameli-Engvall et al., 2006; Exley et al., 2011). In experiments (Mameli-Engvall et al., 2006), the mean number of spikes in WT mice in a burst was 3.1 ± 0.52. In our simulations, the average length was 2.7 ± 0.25 spike per burst, which is within the range observed in the experiments.

Results

With our model, we give an account in silico for the ACh- and nicotine-induced modulations observed in the experiments. We explain and provide mechanisms for several apparently contradictory experimental results. First, systemic KO of ß2-containing nAChRs drastically reduces DA neuron bursting even though the major Glu afferents that have been shown to evoke this bursting stay intact. Second, the most intuitive way to rescue this bursting by reexpressing the nAChRs on VTA DA neurons fails. Third, nAChR re-expression on VTA GABA neurons rescues DA neuron bursting under the influence of ACh input, but nicotinic application results in the opposite changes in VTA DA neuron firing.

Balanced excitatory and inhibitory inputs to DA neurons support their tonic firing in the β2 nAChR knock-out conditions

In animals lacking β2-containing nAChRs, VTA DA neurons were shown to fire at lower frequencies than the controls, and display practically no bursting *in vivo* (see Figs 1,2). Burst firing of VTA DA neurons has been previously, at least in part, attributed to activation of their Glu synaptic inputs (Morikawa et al., 2003; Blythe et al., 2007; Deister et al., 2009). This leads to a question why the knockout of β2 containing nAChRs abolished bursting in DA neurons if their Glu inputs remain intact? Considering that some excitatory inputs to the VTA DA neurons are tonically active (e.g. STN (Wilson et al., 2004)), we modeled the Glu inputs as Poisson-distributed spike trains, which together produce near-tonic activation of NMDA receptors on DA neurons. Simultaneously, the DA neurons receive inhibitory inputs (Paladini and Tepper, 1999; Kaufling et al., 2010), which in the model are provided by population activity of VTA GABA neurons. While Glu inputs alone through NMDA receptor activation can cause increases in DA

neuron firing and bursting, co-activation of GABA receptors can balance the excitation and re-establish low-frequency near-tonic firing (Lobb et al., 2010). This behavior have been reproduced in previous modeling studies (Morozova et al., 2016a). Accounting for the low-rate tonic firing activity of the DA neuron required the GABAR and NMDAR conductances in the model to be set to produce a balance in the GABA and Glu inputs to the DA neuron (Fig. 4). Thus, the model implies that in the β2 nAChR KO conditions the excitatory and inhibitory inputs to VTA DA neurons remain balanced and preserve tonic activity of the neurons.

Intrinsic excitability properties of the DA neuron limit effects of direct excitation via β2-containing nAChRs

The most intuitive explanation of low DA neurons' bursting in β2 nAChR KO mice would be the lack of direct excitation through these receptors on DA neurons. However, targeted re-expression of the receptors on DA neurons does not alleviate low bursting (Fig. 1 green). The firing rate also remains much lower than in the WT conditions. The main effect of this re-expression is that nicotine application produces robust increase in the firing rate of DA neurons (Fig. 2 green), similar to that in WT conditions. However, bursting is not increased during the influence of nicotine (Fig. 2 green), by contrast to that in the WT mice.

Conductance of the nAChR current was set to a low value ($\bar{g}_{AchDA} = 5mS/cm^2$) to reproduce the lack of significant change in the firing rate of the β2DA-VEC (experiment: Fig. 1 green; model: Fig. 5 green) in comparison with the KO case (Experiment: Fig. 1 red; model: Fig. 5 red). For these low conductance values, bursting was also not altered by the direct ACh inputs on the DA neurons. The choice of the conductance value was based on our parametric analysis of its influence on the DA neuron firing rate and bursting included in Extended data (Fig. 5-1). Thus,

the model reproduces experimentally observed invariance of the VTA DA cell activity under the direct nAChR-mediated cholinergic input to the DA neurons.

In addition to the cholinergic input, we were able to account for the effects of the nicotine application. As in the experiments, the firing rate, but not bursting of the DA neuron substantially increases with activation of the β2 receptors for about 300 sec by elevated nicotine concentration (Fig. 6 green). The increase is significant, by contrast to that produced by ACh alone. This simply reflects a greater increase in the nAChR-mediated current by the combination of nicotine and ACh. Desensitization of the receptors will eventually decrease their current, but at a much longer timescale of 1 min.

The explanation for the lack of increase in burstiness during nicotine exposure is that bursting in DA neurons strongly relies on the activation of the NMDA receptor (Overton and Clark, 1992; Chergui et al., 1993; Deister et al., 2009) due to its voltage dependence (magnesium block) (Deister et al., 2009; Ha and Kuznetsov, 2013). By contrast, tonic activation of linear current mediated by the nicotinic receptors is not effective in eliciting bursting in DA neurons. In fact we can think about the nAChR-mediated current as being similar to a slow-varying AMPA input, since both are not-voltage dependent, as opposed to the voltage-rectifying NMDA-synaptic currents. Therefore, even strong continuous increase in the nAChR-mediated current on the VTA DA neuron does not increase its bursting.

Distinct temporal profiles of AChR activation explains opposite effects of endogenous ACh and nicotine on VTA DA neuron firing.

Counter-intuitively when β2-containing nAChRs are re-expressed only on VTA GABA neurons, endogenous ACh input and exogenous nicotinic application results in opposite changes in firing

of VTA DA neurons. In particular, the firing rate and especially bursting of VTA DA neurons are sharply increased after the re-expression of β2 nAChRs on VTA GABA neurons compared to the KO conditions (experiment: Fig. 1; model: Fig. 5 blue vs. red). By contrast, additional agonist effect on these receptors by nicotine causes a decrease in the firing and bursting of the DA neuron (experiment: Fig. 2 blue; model: Fig. 6 blue). While the decrease in the firing caused by nicotine can be intuitively explained by a greater activation of the GABA neurons, which in turn inhibits the DA neurons, the boost in activity of DA neurons produced by ACh is harder to understand. We show that our model is capable to account for these effects in a mechanistic manner.

As before, cholinergic input arriving at the GABA neurons was modeled by a spike train reproducing burstiness of the afferents (see Methods). Following afferent convergence principle, we assumed that a subpopulation of VTA GABA neurons receives common endogenous cholinergic input that activates the β2 nAChRs on these neurons. Previously, we have shown that such common input can synchronize the GABA neurons and functionally invert their inhibitory influence on DA neurons (Morozova et al., 2016a). We showed that a synchronous pulsatile GABA input is able to significantly increase firing rate and burstiness of the DA neurons via dynamical reduction the Ca^{2+} -dependent K^{+} current. This mechanism works here for the influence of ACh inputs through the GABA neurons onto the DA neurons: due to fast, transient activation of nAChRs, cholinergic pulses act as synchronizing inputs to GABA neurons (Fig. 7). The synchronized GABA synaptic input onto the DA neuron acts in turn to increase its firing rate and burstiness. Thus, experimentally observed increases in firing and bursting of the DA neurons that follow nAChRs re-expression on VTA GABA neurons could be mechanistically explained

by changing the level of synchronization in the population of the GABA neurons (Morozova et al., 2016a).

By contrast to the pulsatile activation of nAChRs by ACh afferents, nicotine activates nAChR on GABA neurons tonically and then desensitizes them. This produces an increase in GABA neuron firing rate without synchronizing the neurons (data not shown). This in turn leads to an increase in the tonic component of GABA synaptic activation on DA neurons. Tonic GABA activation on DA neurons leads to a decrease in their firing, which allows us to reproduce the inhibitory influence of nicotine through GABA neurons (Fig. 6 blue; see Fig. 6-1 for parameter dependence).

Co-activation of β2 nAChRs on VTA DA and GABA neurons is required for both ACh and nicotine to boost DA neuron bursting

Under the ACh input, re-expression of β2-containing nAChRs on all VTA neurons elevated firing rate and burstiness of DA neurons to the levels displayed in the WT animals (see Fig 1B). We have reproduced this modulation in the model (Fig. 5 purple). However, this required a modification of the nAChR conductances compared to the above re-expression cases (Table 2). The model shows that the ACh- and nicotine-induced modulations strongly depend on the balance between expression of these receptors on DA and GABA neurons. For example, if we combine the conductances at the values used in the two single re-expression cases, both firing rate and bursting will be very high under the ACh input, but decrease with nicotinic application, which is opposite to experiments. Therefore, nAChR conductance was reduced by a factor of 2.6 on the GABA neurons and increased by a factor of two on the DA neuron. Thus, model calibration predicts that the elevated firing rate and burstiness caused by coexpression of

nAChRs on both the GABA and the DA neurons, although attaining very similar values, rely in a very different mechanism: The firing rate is increased due to a direct ACh-mediated excitation of DA neurons, whereas GABA neuron influence augments bursting.

Nicotine application after re-expression of β2-containing nAChRs on both VTA DA and GABA neurons produced increases in both firing rate and bursting of DA neurons in experiments (Fig. 2, purple). To model this case, nicotinic input was applied to both DA and GABA neurons. Resulting DA neuron firing rate is produced by a competition between nicotine-evoked direct excitation and GABA-mediated inhibition. We used the same parameters as in the case of ACh influence on both neurons above. The overall increase in DA neuron firing rate was achieved due to a stronger direct excitation of DA neurons than their inhibition through GABA neurons by nicotine (Fig. 6 purple). However, as it follows from the case of nAChRs re-expression only on DA neurons, this pathway cannot be implicated in increasing bursting of the DA neurons. The mechanism for increasing bursting combines the increase in direct excitation and GABA neuron-mediated inhibition of DA neurons. We have shown that this combination effectively increases DA neuron bursting as spikes within bursts are more resistant to inhibition than those without (Morozova et al., 2016a; DiVolo et al., n.d.). Thus, increased firing rate and bursting of DA neurons induced by nicotine application through β2-containing nAChRs suggests the convergence of both direct excitation and GABA-mediated inhibition with the latter having a weaker influence.

A combination of nicotinic activation of β2-containing nAChRs on VTA neurons and Glu projections underlies modulation of DA neuron firing in wild type mice

Re-expression of β2-containing nAChRs on all VTA neurons supposedly restores the influence of ACh and nicotine within, but not outside of the VTA. Therefore, some distinctions from firing rates and patterns of DA neurons in WT mice may remain. In the absence of nicotine, the firing rate and bursting of DA neurons in WT mice are not statistically different from that in the whole VTA re-expression case (Fig. 1 black). However, nicotine application increases bursting and firing rate to greater levels in WT compared to the whole VTA re-expression case (Fig. 2 black). In simulations, we use the same conductances of the nAChRs on both DA and GABA neurons as in the double re-expression case above. To account for nicotinic modulation in other brain regions as the nAChRs are preserved throughout the brain, we increase the average frequency of Glu afferents from 50 to 60Hz for the duration of the nicotine injection. The increase caused greater DA neuron firing rates and bursting compared to double re-expression case (Fig. 6 black; compare to purple) during nicotinic excitation of the receptors, matching the experimental results. Therefore, a combination of modulations produced by nicotine inside and outside of the VTA allows us to reproduce the impact of nicotine administration on the firing properties of the VTA DA neurons.

Discussion

The above results provide essential details of how nicotine impacts the drug reinforcement-related circuitry in the VTA. The amplified phasic DA output of the circuit requires concerted activation of β2-nAChRs on both DA and GABA neurons in the VTA (Tolu et al., 2013). Our modeling suggests that direct excitation of DA neurons by endogenous ACh via nAChRs is not enough to increase bursting. In fact, co-activation of GABA neurons via the same receptor activation does not exert the suggested inhibitory influence, but is necessary for bursting. The

mechanism that allows us to reproduce the experimental results is the modulation of synchrony levels in the VTA GABA neural population. Synchronization among GABA neurons produces pulsatile hyperpolarizing input to the DA neurons that increases their firing and bursting (Morozova et al., 2016a). A pulsatile GABA input dynamically reduces long-lasting intrinsic inhibition (Ca^{2+} -dependent K^{+} currents), and the pulsatile pattern of the external inhibition allows the DA neurons to escape it and fire spikes between the pulses. This promotes the occurrence of extra DA neuron spikes via phasic disinhibition. On the contrary, a desynchronized GABA population provides nearly constant level of inhibition to DA neurons, which suppresses their firing. The difference in synchrony can be produced by ACh input vs. nicotinic injection. Due to fast transient activation of β2-nAChRs, ACh pulses can act as synchronizing inputs to these GABA neurons. By contrast, nicotine persistently activates nAChRs, causing an increase in the frequency without synchronizing the GABA population. This study highlights the role of GABA interneurons, and in particular, the temporal pattern of their activity, in the regulation of DA neurons bursting.

Our modeling has reconciled apparent controversies of complex cholinergic and nicotinic modulation of the VTA DA neuron firing rate and pattern. First, systemic KO of β2-nAChRs drastically reduces bursting of DA neurons. DA neuron bursting have been shown to depend on the Glu inputs (Morikawa et al., 2003; Blythe et al., 2007; Deister et al., 2009) and has a major behavioral function as an unexpected reward signal (Schultz, 2002; Tobler et al., 2005). However, Glu inputs to VTA in the β2-nAChRs KO mice likely remain intact and suffer only minor changes in their activity as they are mostly modulated by the α7-containing nAChRs (Koukouli and Maskos, 2015). Further, re-expression of nAChRs within VTA restores high bursting levels. What is the mechanism that allows ACh to modulate bursting of the DA

neurons? Our modeling shows that without β2-nAChRs, Glu excitation of VTA DA neurons remains in balance with inhibition mediated by neighboring VTA GABA neurons. Both neural groups receive partly overlapping Glu projections (Beier et al., 2015), and this may help preserve the balance throughout different behavioral states. ACh inputs to VTA break the inhibition-excitation balance and, consequently, increase VTA DA neuron bursting. This make the motivation and saliency signals carried by DA bursting to be vulnerable to the influence of nicotine and other substances affecting β2-nAChRs.

Second, a straight-forward way to restore DA neuron activity does not work: re-expression of nAChRs on the DA neuron does not elevate its bursting and increases its firing rate only under the influence of nicotine. Why direct excitation through β2-nAChRs does not restore DA neuron activity? The answer may be in the similarity of the β2-nAChRs to other types of excitatory receptors that do not have voltage dependence: When driven by Glu inputs, DA neurons are most responsive to activation of their NMDA receptors (Overton and Clark, 1992; Chergui et al., 1993; Deister et al., 2009). By contrast, AMPA receptors are much less effective in eliciting bursts. The receptor difference that has been shown to be critical is the voltage dependence of the NMDA receptor: it is blocked by magnesium ions at lower voltages (Deister et al., 2009). This blockade allows the cell to repolarize and go into the next oscillation, whereas activation of the AMPA receptor does not allow for the repolarization and block oscillations all together. Similar to AMPA and distinct from NMDA receptors, β2-nAChRs do not have voltage dependence. Therefore, ACh input to DA neurons by itself is not effective in driving their bursting. This direct excitation can, however, significantly increase the DA neuron firing rate, which occurs under the influence of nicotine.

Third, ACh input and nicotinic application result in opposite changes in VTA DA neuron firing when β2-nAChRs are re-expressed only on VTA GABA neurons. In particular, the firing rate and especially bursting of VTA DA neurons are sharply increased after the re-expression compared to the KO conditions. Application of nicotine, by contrast, decreases their firing rate and bursting. How these modulations can be reconciled? Our model uses the difference in the temporal pattern of receptor activation under the influence of ACh input vs. nicotine: While ACh input produces pulsatile activation of the receptor, nicotine-induced activation is continuous and long-lasting. A pulsatile input to the VTA GABA population can synchronize its firing and make its output to the DA neurons pulsatile as well. Again, such pulsatile inhibition of DA neurons may boost their bursting (Morozova et al., 2016a). Therefore, we predict that the opposite influence of ACh and nicotine through β2-nAChRs on GABA neurons is caused by distinct temporal structure of the stimulation: pulsatile vs. continuous.

In the experiments, the modulations of DA neuron firing introduced with re-expression of β2-nAChRs on both DA and VTA GABA neurons closely reproduce that in WT mice under endogenous ACh inputs. However, these double re-expression experiments do not completely reproduce those in the WT mice during nicotine application. In particular, both firing rate and bursting evoked by nicotine are higher in the WT case (Fig. 2 and 6). One possibility is that this difference is due to altered expression of the receptors inside the VTA. It is plausible that the re-expression levels could be different in these conditions. However, the difference between the case of re-expressing the receptors in all VTA neurons and the WT occurs only during nicotine application. Therefore, we assume that this difference is due to the expression of β2-nAChRs outside of the VTA, which is not rescued by the re-expression. We assume that nicotine increases cortical activity in the WT mice greater than in the β2 KO mice consistent with

nicotine-induced activation of β2-nAChRs receptors on deep layer pyramidal neurons (Toyoda, 2018) and on the disinhibitory interneurons in the superficial cortical layers (Koukouli et al., 2017). We reproduced the elevated firing rate and bursting of DA neurons during nicotine application in the WT model with a modest increase in the average firing rate of Glu afferents to the VTA for the duration of nicotine application.

Note that we did not have to assume that the Glu input to the VTA changes its temporal structure under the manipulations performed experimentally. We propose a local VTA circuit mechanism for the changes in the DA cell activity. Previous modeling work has shown that the Glu afferent input that has a bursty temporal structure also increases the burstiness of the DA neuron (Morozova et al., 2016a). It is known that α7-containing nAChRs modulate Glu inputs to the VTA (Schilström et al., 1998, 2000, 2003) and impact DA neuron bursting in a subtle manner (Mameli-Engvall et al., 2006): β2-nAChRs appeared to exert an overwhelming control over all bursting under ACh and nicotine, while the α7-nAChRs manipulations in β2 intact animals affected bursting in a subpopulation of DA neurons with relatively low mean firing rates. These previous results suggest that a7-nAChRs have impact on bursting, but in a manner that is strongly controlled by the β2-nAChRs. Previous data suggests that deletion of α4 or α6 subunits do not cause significant changes in firing and bursting of DA neurons (Exley et al., 2011). Therefore, different subtypes of nAChRs may control different sources of DA neuron bursting and, therefore, motivational and saliency signals associated with this bursting. However, in the experiments considered in the present study, the α7-nAChRs were not modulated. Hence, we must conclude that the changes we see in DA cell activity are due to β2-nAChR effects.

Previous results suggested that the co-activation of VTA DA and GABA neurons is required for the habit-forming effects of nicotine. How does the mechanism revealed in this

paper explain the requirement of GABA neuron activation? The co-excitation of DA and GABA neurons constitute the conditions in which DA neuron bursting is maximized in the model. Indeed, excitation of DA neurons only can elevate their firing rate, but does not group spikes into bursts. We predict that the additional excitation of the GABA neurons increases bursting it two ways: First, the tonic component of the inhibition mostly cancels the spikes without rather than within bursts. This mechanism contributes most during nicotine application. Second, excitation of GABA neurons by common inputs may also synchronize their firing and further promote bursting by providing pulsatile inhibition to DA neurons. This is a mechanism that provides background ACh- but not nicotine-driven DA neuron bursting because nicotine blunts the temporal profile of β2-nAChRs activation, and, thus, destroys synchronous pulses of GABA inhibition. Therefore, co-activation of DA and GABA neurons is required for DA neuron bursting and, thus, motivation and saliency signals carried by these bursts, which are hijacked by nicotine and other addictive drugs.

References

Bayer HM, Glimcher PW (2005) Midbrain Dopamine Neurons Encode a Quantitative Reward Prediction Error Signal. Neuron 47:129–141.

Beier KT, Steinberg EE, DeLoach KE, Xie S, Miyamichi K, Schwarz L, Gao XJ, Kremer EJ, Malenka RC, Luo L (2015) Circuit Architecture of VTA Dopamine Neurons Revealed by Systematic Input-Output Mapping. Cell 162:622–634.

Benowitz NL (2009) Pharmacology of nicotine: addiction, smoking-induced disease, and therapeutics. Annu Rev Pharmacol Toxicol 49:57–71.

Benowitz NL (2010) Nicotine Addiction Schwartz RS, ed. New England Journal of Medicine 362:2295–2303.

Blythe SN, Atherton JF, Bevan MD (2007) Synaptic activation of dendritic AMPA and NMDA receptors generates transient high-frequency firing in substantia nigra dopamine neurons in vitro. J Neurophysiol 97:2837–2850.

490 Bocklisch C, Pascoli V, Wong JCY, House DRC, Yvon C, de Roo M, Tan KR, Luscher C (2013)
491 Cocaine Disinhibits Dopamine Neurons by Potentiation of GABA Transmission in the
492 Ventral Tegmental Area. Science 341:1521–1525.

493 CDCTobaccoFree (2017) Tobacco-Related Mortality. Centers for Disease Control and
494 Prevention Available at:
495 https://www.cdc.gov/tobacco/data_statistics/fact_sheets/health_effects/tobacco_related_
496 mortality/index.htm [Accessed March 7, 2019].

497 Changeux J-P (2010) Nicotine addiction and nicotinic receptors: lessons from genetically
498 modified mice. Nature Reviews Neuroscience 11:389–401.

499 Chergui K, Charléty PJ, Akaoka H, Saunier CF, Brunet JL, Buda M, Svensson TH, Chouvet G
500 (1993) Tonic activation of NMDA receptors causes spontaneous burst discharge of rat
501 midbrain dopamine neurons in vivo. Eur J Neurosci 5:137–144.

502 Deister CA, Teagarden MA, Wilson CJ, Paladini CA (2009) An intrinsic neuronal oscillator
503 underlies dopaminergic neuron bursting. J Neurosci 29:15888–15897.

504 DiVolo M, Morozova E, Lapish C, Kuznetsov A, Gutkin B (n.d.) Circuit-level Mechanisms of
505 EtOH-dependent dopamine release. European J Neuroscience; Under revision.

506 Durand-de Cuttoli R, Mondoloni S, Marti F, Lemoine D, Nguyen C, Naudé J, d'Izarny-Gargas
507 T, Pons S, Maskos U, Trauner D, Kramer RH, Faure P, Mourot A (2018) Manipulating
508 midbrain dopamine neurons and reward-related behaviors with light-controllable
509 nicotinic acetylcholine receptors. eLife 7 Available at:
510 https://elifesciences.org/articles/37487 [Accessed March 6, 2019].

511 Everitt BJ, Robbins TW (2005) Neural systems of reinforcement for drug addiction: from actions
512 to habits to compulsion. Nature Neuroscience 8:1481–1489.

513 Exley R, Maubourguet N, David V, Eddine R, Evrard A, Pons S, Marti F, Threlfell S, Cazala P,
514 McIntosh JM, Changeux J-P, Maskos U, Cragg SJ, Faure P (2011) Distinct contributions
515 of nicotinic acetylcholine receptor subunit 4 and subunit 6 to the reinforcing effects of
516 nicotine. Proceedings of the National Academy of Sciences 108:7577–7582.

517 Faure P, Tolu S, Valverde S, Naudé J (2014) Role of nicotinic acetylcholine receptors in
518 regulating dopamine neuron activity. Neuroscience 282:86–100.

519 Garzón M, Vaughan RA, Uhl GR, Kuhar MJ, Pickel VM (1999) Cholinergic axon terminals in
520 the ventral tegmental area target a subpopulation of neurons expressing low levels of the
521 dopamine transporter. J Comp Neurol 410:197–210.

522 Grace AA (1991) Phasic versus tonic dopamine release and the modulation of dopamine system
523 responsivity: a hypothesis for the etiology of schizophrenia. Neuroscience 41:1–24.

524 Grace AA, Bunney BS (1984) The control of firing pattern in nigral dopamine neurons: burst
525 firing. J Neurosci 4:2877–2890.

526 Graupner M, Maex R, Gutkin B (2013) Endogenous Cholinergic Inputs and Local Circuit
527 Mechanisms Govern the Phasic Mesolimbic Dopamine Response to Nicotine Friston KJ,
528 ed. PLoS Computational Biology 9:e1003183.

529 Ha J, Kuznetsov A (2013) Interaction of NMDA Receptor and Pacemaking Mechanisms in the
530 Midbrain Dopaminergic Neuron Mansvelder HD, ed. PLoS ONE 8:e69984.

531 Kaufling J, Veinante P, Pawlowski SA, Freund-Mercier M-J, Barrot M (2010) γ-Aminobutyric
532 Acid Cells with Cocaine-Induced ΔFosB in the Ventral Tegmental Area Innervate
533 Mesolimbic Neurons. Biological Psychiatry 67:88–92.

534 Kayama Y, Ohta M, Jodo E (1992) Firing of "possibly" cholinergic neurons in the rat
535 laterodorsal tegmental nucleus during sleep and wakefulness. Brain Res 569:210–220.

536 Keiflin R, Janak PH (2015) Dopamine Prediction Errors in Reward Learning and Addiction:
537 From Theory to Neural Circuitry. Neuron 88:247–263.

538 Klink R, de Kerchove d'Exaerde A, Zoli M, Changeux JP (2001) Molecular and physiological
539 diversity of nicotinic acetylcholine receptors in the midbrain dopaminergic nuclei. J
540 Neurosci 21:1452–1463.

541 Koob GF, Sanna PP, Bloom FE (1998) Neuroscience of addiction. Neuron 21:467–476.

542 Koukouli F, Maskos U (2015) The multiple roles of the α7 nicotinic acetylcholine receptor in
543 modulating glutamatergic systems in the normal and diseased nervous system.
544 Biochemical Pharmacology 97:378–387.

545 Koukouli F, Rooy M, Tziotis D, Sailor KA, O'Neill HC, Levenga J, Witte M, Nilges M,
546 Changeux J-P, Hoeffer CA, Stitzel JA, Gutkin BS, DiGregorio DA, Maskos U (2017)
547 Nicotine reverses hypofrontality in animal models of addiction and schizophrenia. Nature
548 Medicine 23:347–354.

549 Koyama Y, Jodo E, Kayama Y (1994) Sensory responsiveness of "broad-spike" neurons in the
550 laterodorsal tegmental nucleus, locus coeruleus and dorsal raphe of awake rats:
551 implications for cholinergic and monoaminergic neuron-specific responses. Neuroscience
552 63:1021–1031.

553 Lobb CJ, Wilson CJ, Paladini CA (2010) A Dynamic Role for GABA Receptors on the Firing
554 Pattern of Midbrain Dopaminergic Neurons. Journal of Neurophysiology 104:403–413.

555 Lodge DJ, Grace AA (2006) The Hippocampus Modulates Dopamine Neuron Responsivity by
556 Regulating the Intensity of Phasic Neuron Activation. Neuropsychopharmacology
557 31:1356–1361.

558 Lüscher C, Ungless MA (2006) The Mechanistic Classification of Addictive Drugs. PLoS
559 Medicine 3:e437.

560 Mameli-Engvall M, Evrard A, Pons S, Maskos U, Svensson TH, Changeux J-P, Faure P (2006)
561 Hierarchical Control of Dopamine Neuron-Firing Patterns by Nicotinic Receptors.
562 Neuron 50:911–921.

563 Mansvelder HD, Keath JR, McGehee DS (2002) Synaptic mechanisms underlie nicotine-induced
564 excitability of brain reward areas. Neuron 33:905–919.

565 Mao D, Gallagher K, McGehee DS (2011) Nicotine potentiation of excitatory inputs to ventral
566 tegmental area dopamine neurons. J Neurosci 31:6710–6720.

567 Marti F, Arib O, Morel C, Dufresne V, Maskos U, Corringer P-J, de Beaurepaire R, Faure P
568 (2011) Smoke extracts and nicotine, but not tobacco extracts, potentiate firing and burst
569 activity of ventral tegmental area dopaminergic neurons in mice.
570 Neuropsychopharmacology 36:2244–2257.

571 Morikawa H, Khodakhah K, Williams JT (2003) Two intracellular pathways mediate
572 metabotropic glutamate receptor-induced Ca2+ mobilization in dopamine neurons. J
573 Neurosci 23:149–157.

574 Morozova EO, Myroshnychenko M, Zakharov D, di Volo M, Gutkin B, Lapish CC, Kuznetsov
575 A (2016a) Contribution of synchronized GABAergic neurons to dopaminergic neuron
576 firing and bursting. Journal of Neurophysiology 116:1900–1923.

577 Morozova EO, Zakharov D, Gutkin BS, Lapish CC, Kuznetsov A (2016b) Dopamine Neurons
578 Change the Type of Excitability in Response to Stimuli Blackwell KT, ed. PLOS
579 Computational Biology 12:e1005233.

580 Naudé J, Tolu S, Dongelmans M, Torquet N, Valverde S, Rodriguez G, Pons S, Maskos U,
581 Mourot A, Marti F, Faure P (2016) Nicotinic receptors in the ventral tegmental area
582 promote uncertainty-seeking. Nature Neuroscience 19:471–478.

583 Nestler EJ, Carlezon WA (2006) The mesolimbic dopamine reward circuit in depression. Biol
584 Psychiatry 59:1151–1159.

585 Overton P, Clark D (1992) Iontophoretically administered drugs acting at the N-methyl-D-
586 aspartate receptor modulate burst firing in A9 dopamine neurons in the rat. Synapse
587 10:131–140.

588 Paladini CA, Tepper JM (1999) GABAA and GABAB antagonists differentially affect the firing
589 pattern of substantia nigra dopaminergic neurons in vivo. Synapse 32:165–176.

590 Picciotto MR, Zoli M, Rimondini R, Léna C, Marubio LM, Pich EM, Fuxe K, Changeux J-P
591 (1998) Acetylcholine receptors containing the β2 subunit are involved in the reinforcing
592 properties of nicotine. Nature 391:173–177.

593 Redgrave P, Gurney K (2006) The short-latency dopamine signal: a role in discovering novel
594 actions? Nature Reviews Neuroscience 7:967–975.

595 Role L, Kandel E (2008) Nicotinic Acetylcholine Receptors: From Molecular Biology to
596 Cognition. Neuron 58:847–849.

597 Sakai K (2012) Discharge properties of presumed cholinergic and noncholinergic laterodorsal
598 tegmental neurons related to cortical activation in non-anesthetized mice. Neuroscience
599 224:172–190.

600 Schilström B, Fagerquist MV, Zhang X, Hertel P, Panagis G, Nomikos GG, Svensson TH (2000)
601 Putative role of presynaptic alpha7* nicotinic receptors in nicotine stimulated increases
602 of extracellular levels of glutamate and aspartate in the ventral tegmental area. Synapse
603 38:375–383.

604 Schilström B, Rawal N, Mameli-Engvall M, Nomikos GG, Svensson TH (2003) Dual effects of
605 nicotine on dopamine neurons mediated by different nicotinic receptor subtypes. Int J
606 Neuropsychopharmacol 6:1–11.

607 Schilström B, Svensson HM, Svensson TH, Nomikos GG (1998) Nicotine and food induced
608 dopamine release in the nucleus accumbens of the rat: Putative role of α7 nicotinic
609 receptors in the ventral tegmental area. Neuroscience 85:1005–1009.

610 Schultz W (2002) Getting formal with dopamine and reward. Neuron 36:241–263.

611 Steffensen SC, Bradley KD, Hansen DM, Wilcox JD, Wilcox RS, Allison DW, Merrill CB,
612 Edwards JG (2011) The role of connexin-36 gap junctions in alcohol intoxication and
613 consumption. Synapse 65:695–707.

614 Taly A, Corringer P-J, Guedin D, Lestage P, Changeux J-P (2009) Nicotinic receptors: allosteric
615 transitions and therapeutic targets in the nervous system. Nature Reviews Drug Discovery
616 8:733–750.

617 Tobler PN, Fiorillo CD, Schultz W (2005) Adaptive coding of reward value by dopamine
618 neurons. Science 307:1642–1645.

619 Tolu S et al. (2013) Co-activation of VTA DA and GABA neurons mediates nicotine
620 reinforcement. Molecular Psychiatry 18:382–393.

621 Toyoda H (2018) Nicotine facilitates synaptic depression in layer V pyramidal neurons of the
622 mouse insular cortex. Neuroscience Letters 672:78–83.

623 Wilson CJ, Weyrick A, Terman D, Hallworth NE, Bevan MD (2004) A Model of Reverse Spike
624 Frequency Adaptation and Repetitive Firing of Subthalamic Nucleus Neurons. Journal of
625 Neurophysiology 91:1963–1980.

626

627

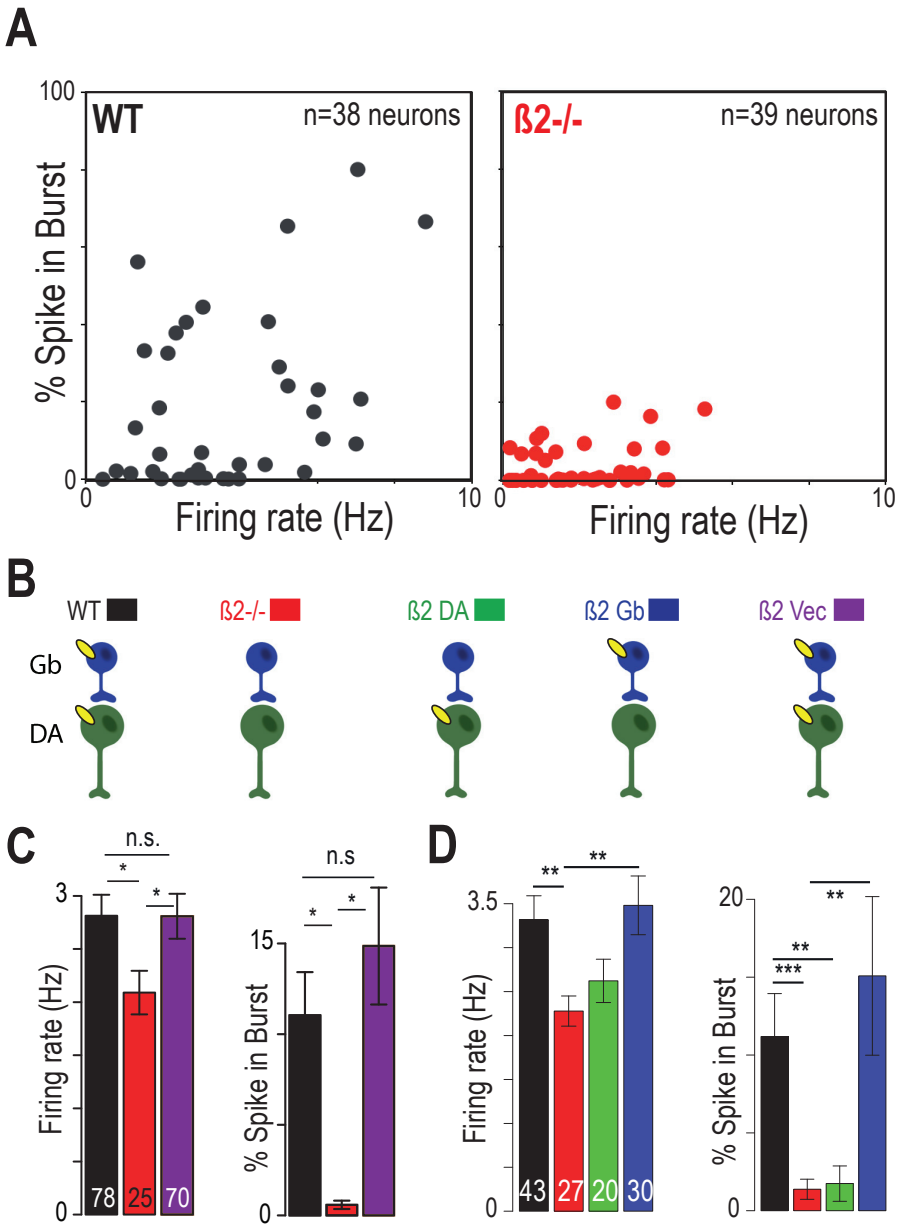

Figure 1. Quantification of firing rate and pattern of the VTA DA neurons in wild type (WT, black), after systemic deletion of β2-containing nAChRs (red), and their subsequent re-expression on VTA DA (green), VTA GABA (blue), and on both neurons (purple). (A) Mean

firing frequency (Hz) against percentage of spikes within a burst (%SWB) for n = 38 and 39 individual cells in WT and β2 KO mice. Systemic deletion of β2-containing nAChR decreases both DA neuron firing rate and bursting compared to WT (see also C and D). (B) Various KO and re-expression cases that have been used to analyze the role of β2-containing nAChRs in the VTA (see methods and C, D)). (C) lentiviral re-expression of β2 subunit in the VTA of ß2 KO mice using a ubiquitous mouse phosphoglycerate kinase (PGK) promoter (β2 Vec) restores firing rate and bursting (Data modified from **(Naudé et al., 2016)**). (D) Comparison of firing rate and bursting in WT (black), β2 KO mice ($\beta2^{-/-}$, red) and mice with re-expression of β2 in a specific neuronal population. Cre recombinase-activated lentiviral expression vector were used to drive specific β2*-nAChR re-expression in DA or GABAergic neurons of the VTA of DAT Cre mice (β2 DA, green), GAD67 Cre mice (β2 Gb, red). (Data from (Tolu et al., 2013))

644

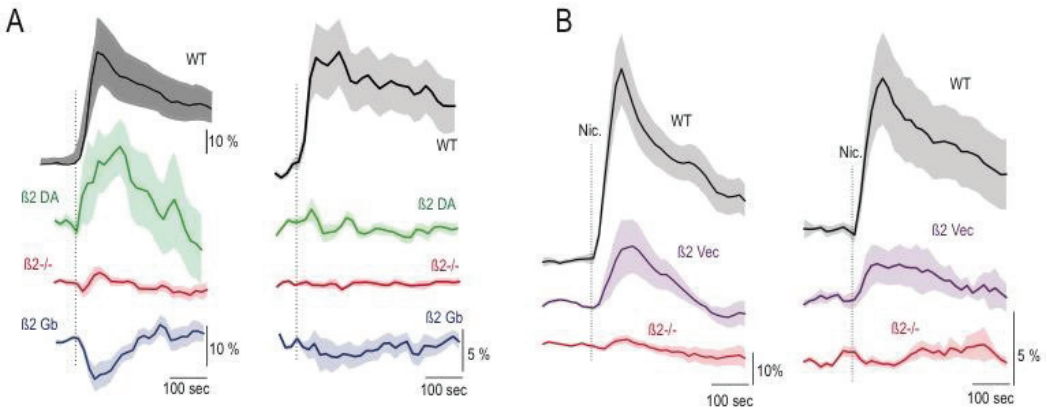

645

646 Figure 2. Comparison of the nicotine-elicited modifications of the firing rate (left) and %SWB
647 (right) in VTA DA neurons in in two set of experiments (A) β2 DA vector (green) and β2 Gb
648 vector (blue) compared to wild type (black) and β2-/- (red) mice (Data modified from (Tolu et
649 al., 2013)). (B) β2-Vec (purple) compared to wild type (black) and β2-/- (red) mice (Data
650 modified from (Naudé et al., 2016)). Vertical dashed line indicates the nicotine injection.

651

652

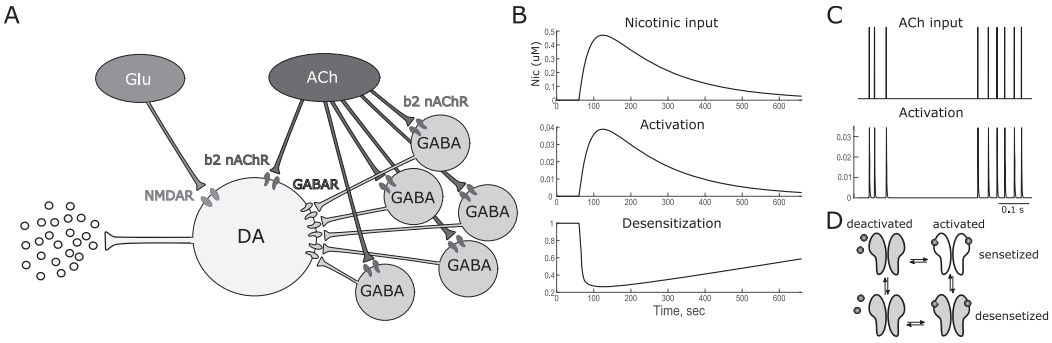

653

654 Figure 3. Schematic of the model. (A) Afferent inputs and microcircuitry of the VTA. (B) Time

655 course of the nicotine concentration and subsequent activation and desensitization of nAChRs.

656 (C) Temporal profile of ACh input and subsequent activation of nAChRs (D) State transitions of

657 the nAChRs.

658

659

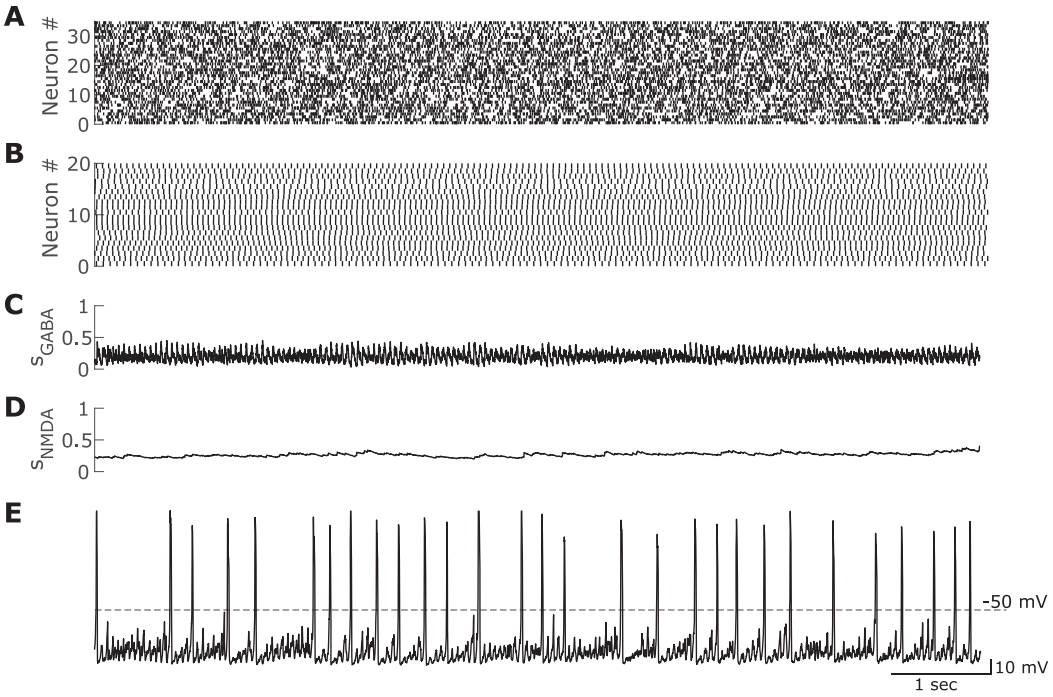

Figure 4. The rate and regularity of the DA neuron firing receiving asynchronous synaptic Glu and GABA inputs. (A) Glu raster. (B) GABA raster. (C) Activation of the GABAR on the DA neuron. (D) Activation of the NMDAR on the DA neuron. (E) The voltage of the DA neuron. Note the high regularity of DA neuron firing.

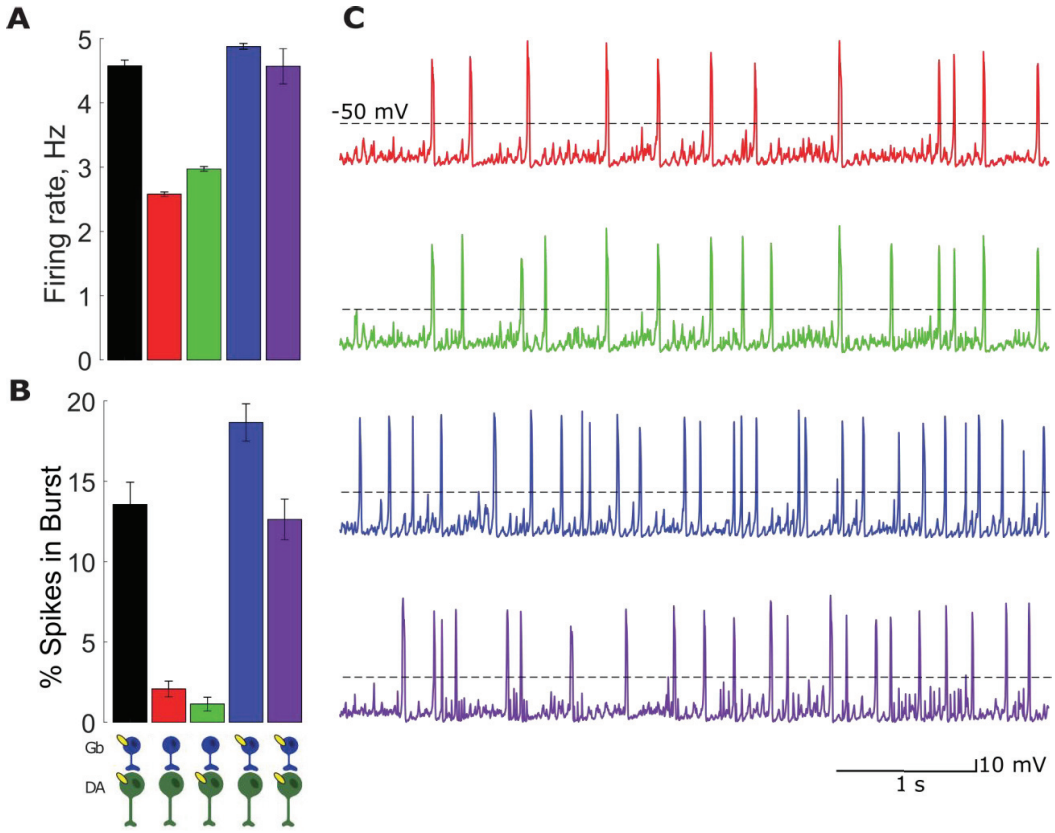

Figure 5. Quantification of spontaneous firing of simulated DA neurons. (A) Bar-plot representation of the mean basal firing rate, represented as means±s.e.m, WT case (black), KO (red), β2-containing nAChRs on DA neurons (green), the nAChRs on GABA neurons (blue) and the nAChRs on DA and GABA neurons (purple). (B) and mean %SWB B) Bar-plot representation of the mean %SWB, represented as means±s.e.m, KO (red), the nAChRs on DA neurons (green), the nAChRs on GABA neurons (blue) and the nAChRs on DA and GABA neurons (purple). (C) Example voltage traces of simulated DA neurons under 4 different conditions indicated in (A) and (B). Colors of the voltage traces matches colors of the bars. Inclusion of nAChR-mediated ACh current to GABA neurons significantly increased DA neuron

677 firing and bursting similarly to the experiment (Tolu et al., 2013). See extended data Fig. 6-1 for
678 parametric analysis.
679

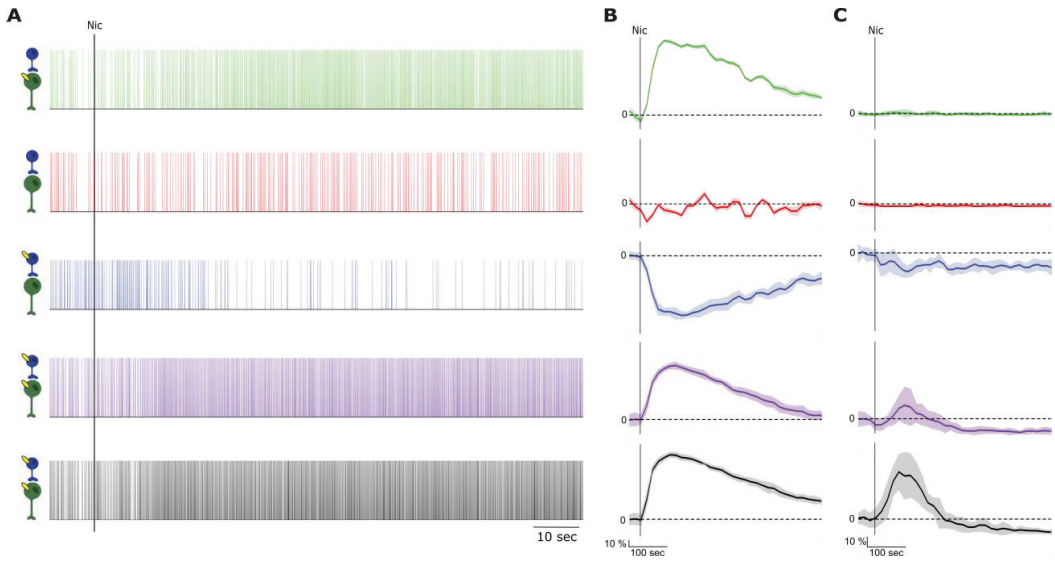

Figure 6. Nicotine-elicited changes in firing rate and burstiness of simulated DA neuron. (A) Raster plots of DA neuron firing in response to nicotine, KO (red), β2-containing nAChRs on DA neurons (green), the nAChRs on GABA neurons (blue), the nAChRs on DA and GABA neurons (purple), and WT case (black). (B) and (C) Nicotine-elicited changes in firing rate (B) and %SWB (C) of simulated DA neurons in response to nicotine. Vertical black line shows the onset of the nicotinic input. There is no change in DA neurons firing or bursting in response to nicotine if both DA or GABA neurons lack the receptors (red). Nicotine increases DA neuron firing if β2-nAChR is added only to DA neuron (green). Oppositely, it decreases DA neuron firing and bursting if β2-nAChR is added only to GABA neurons (blue). Interestingly, nicotine increases DA neuron firing and bursting if β2-nAChRs are added to both neurons (purple). Nicotine elicits even greater response in WT-like case, due to the nicotine-elicited increase in frequency of Glu inputs to the DA neurons (black). See extended data Fig. 6-1 for parametric analysis.

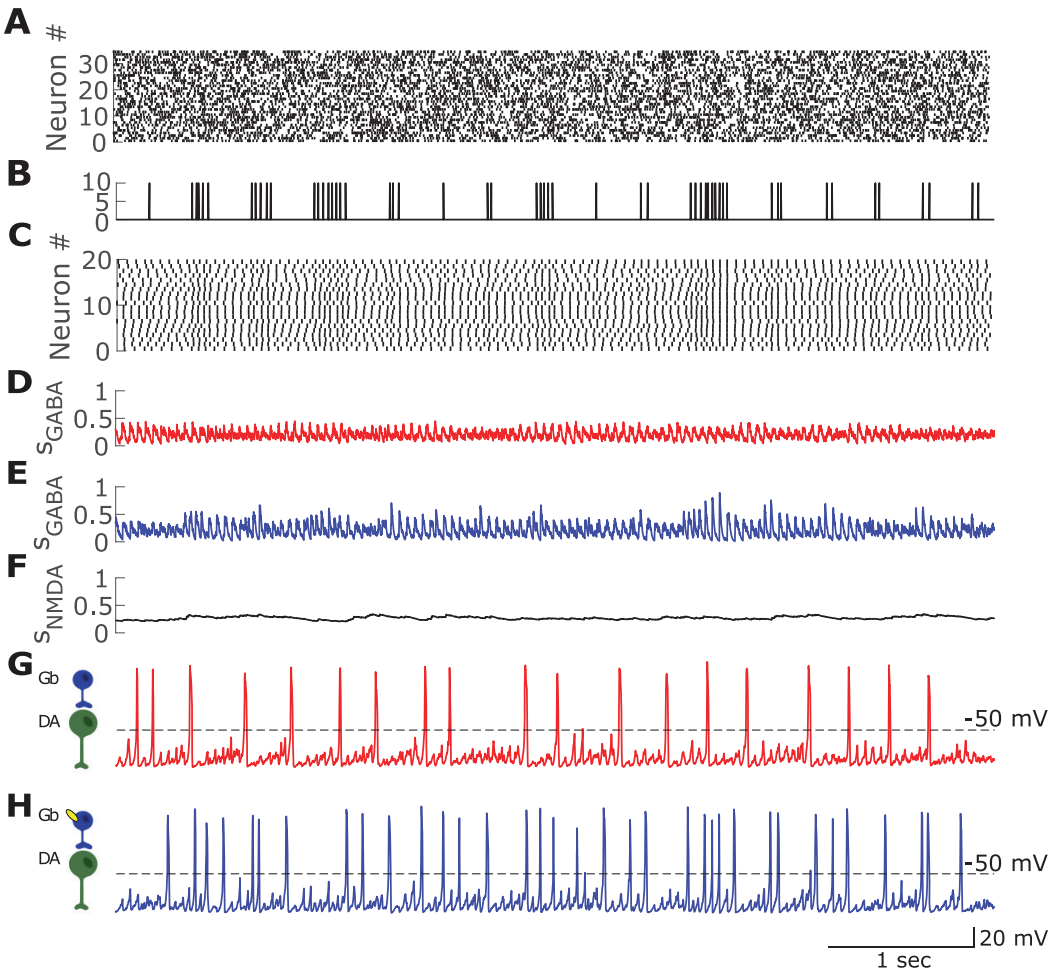

Figure 7. Bursty pulsatile cholinergic input transiently synchronizes GABA neurons. Synchronous GABA input evokes additional DA spikes and increases DA neuron burstiness. (A) Raster of Glu neurons. (B) ACh input. (C) Raster of VTA GABA neurons. (D) and (E) show the cumulative activation variable of the GABAR current on DA neurons without (red) and with (blue) ACh input. (F) shows the activation variable of the NMDAR current on the DA neuron. Note the lack of significant variations. (G) and (H) are voltages of the DA neuron in the cases

they receive GABAR activation from panel (D) or (E) respectively. Note a greater number of spikes grouped in bursts when the nAChR is added to the GABA neurons (blue).

Extended Data

Table 1-1: Model parameters

Parameter	Description	Value
c_m	Membrane capacitance	$1\mu F / cm^2$
$\bar{g}_K$	Potassium conductance	$1mS / cm^2$
$\bar{g}_{Ca}$	Calcium conductance	$2.5mS / cm^2$
$\bar{g}_{KCa}$	Calcium-dependent potassium conductance	$7.8mS / cm^2$
$\bar{g}_{sNa}$	Subthreshold sodium conductance	$0.13mS / cm^2$
g_{leak}	Leak conductance	$0.18mS / cm^2$
E_K	Potassium reversal potential	$-90mV$
E_{Ca}	Calcium reversal potential	$50mV$
E_{Na}	Sodium reversal potential	$55mV$
E_{leak}	Leak reversal potential	$-35mV$
E_{NMDA}	NMDA reversal potential	$0mV$
E_{AMPA}	AMPA reversal potential	$0mV$
E_{GABA}	GABA reversal potential	$-90mV$
τ_{aact}	AMPA receptor activation time	$1ms$
τ_{adeact}	AMPA receptor deactivation time	$1.6ms$

τ_{ades}	AMPA receptor desensitization time	6.1*ms*
$\tau_{adesrel}$	AMPA receptor release from desensitization time	40*ms*
τ_{nact}	NMDA receptor activation time	7*ms*
τ_{ndeact}	NMDA receptor deactivation time	170*ms*
τ_{gact}	GABA receptor activation time	0.08*ms*
τ_{gdeact}	GABA receptor deactivation time	10*ms*

Parametric analysis of DA neuron firing

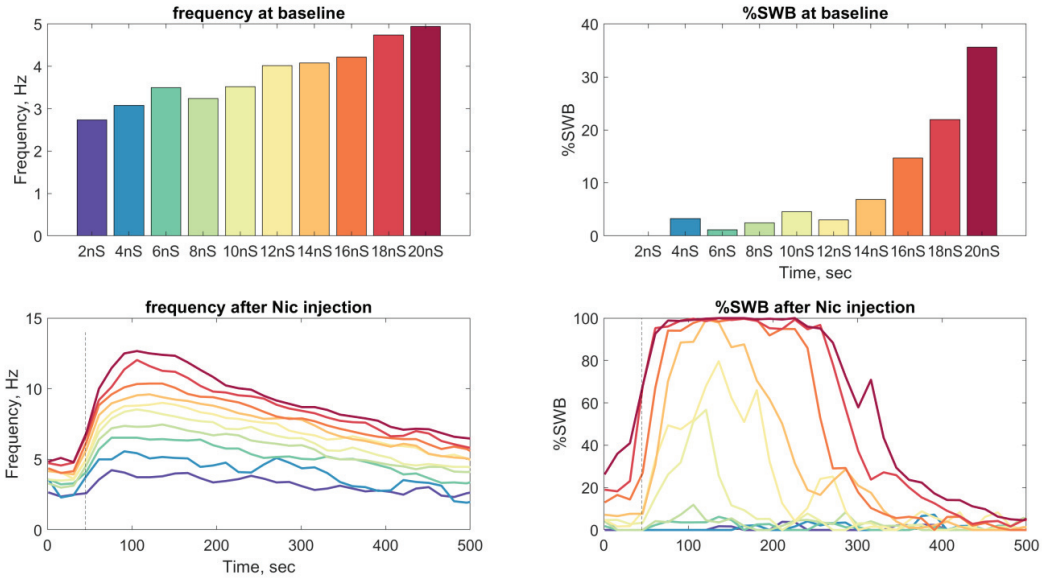

Figure 5-1: Parametric analysis of DA neuron responses to ACh and nicotinic inputs for different maximal conductances of nAChR current (mimicking different levels of expression of nAChRs) on DA neurons. The range of low nAChR conductances gives a good correspondence with the experimental data.

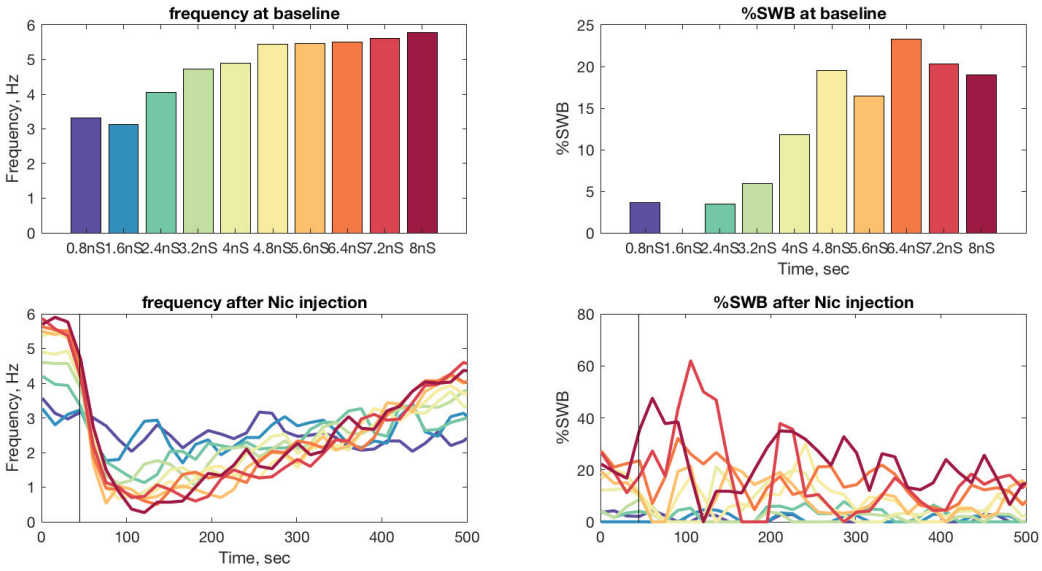

732

733 Figure 6-1: Parametric analysis of DA neuron responses to ACh and nicotinic inputs for different
734 maximal conductances of nAChR current (mimicking different levels of expression of nAChRs)
735 on GABA neurons. The range of low nAChR conductances on GABA neurons gives a good
736 correspondence with the experimental data.